The data processing of the temporarily and spatially mixed modulated polarization interference imaging spectrometer

Xiaohua Jian, [1, 2] Chunmin Zhang, [1, 2*] Lin Zhang, [1, 2] and Baochang Zhao[3]

[1]*School of Science, Xi'an Jiaotong University, Xi'an 710049, China*
[2]*Non-equilibrium Condensed Matter and Quantum Engineering Laboratory, the Key Laboratoryof Ministry of Education, Xi'an 710049 PR China*
[3]*Xi'an Institute of Optics and Precision Mechanics, Academia Sinica, Xi'an 710119, China*
**zcm@mail.xjtu.edu.cn*

Abstract: Based on the basic imaging theory of the temporally and spatially mixed modulated polarization interference imaging spectrometer (TSMPIIS), a method of interferogram obtaining and processing under polychromatic light is presented. Especially, instead of traditional Fourier transform spectroscopy, according to the unique imaging theory and OPD variation of TSMPIIS, the spectrum is reconstructed respectively by wavelength. In addition, the originally experimental interferogram obtained by TSMPIIS is processed in this new way, the satisfying result of interference data and reconstructed spectrum prove that the method is very precise and feasible, which will great improve the performance of TSMPIIS.

OCIS codes: (300.6300) Spectroscopy, Fourier transforms; (070.0070) Fourier optics and signal processing; (120.6200) Spectrometers and spectroscopic instrumentation;

References and links

1. R. J. Bell, *Introductory to Fourier Transform Spectroscopy* (Academic, 1972)
2. M. J. Persky, "A review of spaceborne Fourier transform spectrometer for remote sensing," Rev. Sci. Instrum. **66**(10), 4763–4793 (1995).
3. K. D. Möller, "Wave-front-dividing array interferometer without moving parts for real-time spectroscope from the IR to the UV," Appl. Opt. **34**(9), 1493–1501 (1995).
4. J. B. Rafert, R. G. Sellar, and J. H. Blatt, "Monolithic Fourier transform imaging spectrometer," Appl. Opt. **34**(31), 7228–7230 (1995).
5. P. D. Matthew, and A. K. Mohammad, "Solid-block stationary Fourier-transform spectrometer," Appl. Opt. **31**, 6096–6101 (1992).
6. W. H. Smith, and P. D. Hammer, "Digital array scanned interferometer: sensors and results," Appl. Opt. **35**(16), 2902–2909 (1996).
7. C. M. Zhang, B. Xiangli, and B. C. Zhao, "A static polarization imaging spectrometer based on a Savart polariscope," Opt. Commun. **203**(1-2), 21–26 (2002).
8. C. M. Zhang, B. Xiangli, and B. C. Zhao, "Analysis of the modulation depth affected by the polarization orientation in polarization interference imaging spectrometers," Opt. Commun. **227**(4-6), 221–225 (2003).
9. C. M. Zhang, B. C. Zhao, and B. Xiangli, "Wide-field-of-view polarization interference imaging spectrometer," Appl. Opt. **43**(33), 6090–6094 (2004).
10. C. M. Zhang, B. Xiangli, and B. C. Zhao, "Permissible deviations of the polarization orientation in the polarization imaging spectrometer," J. Opt. A. **6**, 815–817 (2004).
11. C. M. Zhang, X. G. Yan, and B. C. Zhao, "A novel model for obtaining interferogram and spectrum based on the temporarily and spatially mixed modulated polarization interference imaging spectrometer," Opt. Commun. **281**, 2050–2056 (2008).
12. X. H. Jian, and C. M. Zhang, "Wide-spectrum reconstruction method for birefringence interference imaging spectrometer," Opt. Lett. (to be published).
13. L. Wu, C. M. Zhang, and B. C. Zhao, "Analysis of the lateral displacement and optical path difference in wide-field-of-view polarization interference imaging spectrometer," Opt. Commun. **273**(1), 67–73 (2007).

1. Introduction

The classical interference imaging spectrometer is based on a scanning Michelson interferometer, called TMIIS (temporarily modulated interference imaging spectrometer) [1,2]. It has a moving mirror to vary optical path difference at several moments, and requires a

#117640 - $15.00 USD Received 24 Sep 2009; revised 13 Jan 2010; accepted 13 Jan 2010; published 5 Mar 2010

precise scanning mechanism and highly stable design which implies high cost and substantial bulk. The drawbacks of this traditional instrument with scanning parts encouraged the development of static systems SMIIS (spatially modulated interference imaging spectrometer) [3–6]. Most of these devices are based on the lateral shearing interference such as the Sagnac interferometer. But due to the serious restriction of pre-aperture, the optical throughput of SMIIS usually is very low, which produces the data interact and a low signal noise ratio. So around 2000s the novel TSMPIIS is firstly introduced [7–9], it throws off the fore-aperture of the Beam-splitter, replaced by the system field view stop, which obviously increases the optical throughput, widens the field of view, and simplifies the instrumental structure. It can get target's two-dimensional spatial information and one-dimensional spectral information which made it very valuable in the field of space remote sensing, resource investigation, environment observation, military scout, and weak signal measurement, etc.

But on the other hand, because TSMPIIS is based on a birefringence interferometer, and don't have a fore-slit, it is very complex to process the detected information. For taking full use of TSMPIIS, this paper emphasizes on the TSMPIIS special interferogram forming, obtaining and processing method, and uses a novel algorithm birefringence interference transform to reconstruct spectrum which makes it easy to handle this kind of instruments.

2. TSMPIIS

Figure 1 shows the optical diagram of the TSMPIIS [7,10]. It consists of polarized interferometer (polarizer P1, Savart plates and analyzer P2), imaging lens, and detector. The key component in the spectrometer is a Savart polariscope. The Savart polariscope consists of two identical uniaxial crystals which are cut so that their optical axes are aligned at 45 degree to the optical axis of the system. The optical axis of the second crystal is perpendicular to the first one, with their principal section crossed. Firstly, an incident beam is polarized by linear polarizer P1 and split into two polarized components and sheared laterally by Savart polariscope. Then analyzer P2 is used to make two components interfere, and the convex lens is employed to image the interference fringes and target image onto the detector.

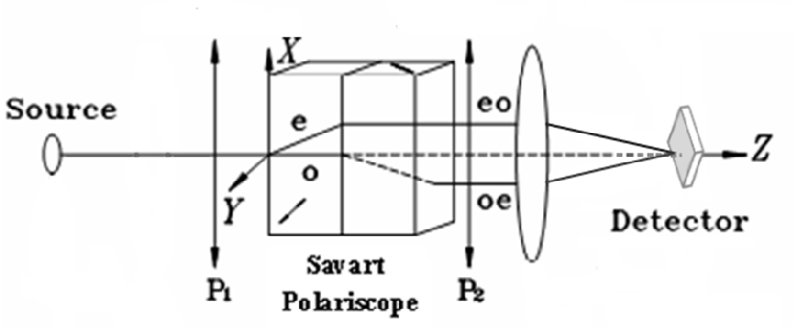

Fig. 1. Optical diagram of the STMPIIS

3. The interferogram forming principle of the TSMPIIS

Generally, because TSMPIIS is equipped on satellite or aircraft, the distance between the targets and TSMPIIS is very huge compared with the size of the instrument or target plots, the incident angle of each target plot can be considered as a constant at one moment. Hereby, the image of every target plot in the detector plane is only one pixel image, and all target plots in the field of view are imaged on the detector simultaneously, just like shown in Fig. 2. When the

#117640 - $15.00 USD Received 24 Sep 2009; revised 13 Jan 2010; accepted 13 Jan 2010; published 5 Mar 2010

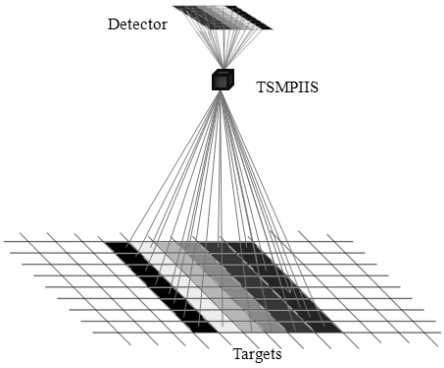

Fig. 2. Field of view of TSMPIIS

TMSPIIS moves over the whole area, every plot experiences the process that the incident angle changes from maximum, zero, finally to negative maximum. At the same time, the detector records the various interference intensities of every plot. Thereby, the whole interferogram data of a target have to be picked out from a series CCD images respectively and organize them regularly. This is the basic work model of TSMPIIS, which is named as temporarily and spatially mixed model [11].

4. The optical path difference of STMPIIS

When an incident beam passes through STMPIIS, it is divided into two beams, and the optical path difference (OPD) between them is [12]:

$$\Delta = t\left[\frac{a^2-b^2}{a^2+b^2}(\cos\omega+\sin\omega)\sin i+\frac{a^2(a^2-b^2)}{\sqrt{2}(a^2+b^2)^{3/2}}(\cos^2\omega-\sin^2\omega)\sin^2 i+\cdots\right] \quad (1)$$

where $a = 1/n_e$, $b = 1/n_o$, n_o and n_e are ordinary and extraordinary refractive indices, t is the thickness of the single Savart plate, i is the incidence angle, and ω is the angle between the plane of incidence and the principle section of Savart plate.

Take the Sarnoff CAM512 CCD as the detector, which utilizes 512 x 512 sensors with 18 x 18 μm pixels, a 0.6328 μm He-Ne Laser as monochromatic source and the field of view is 3°, then according to Eq. (1) the OPD is shown as Fig. 3. The OPD is linear-distributed and uniformly-spaced. In this situation, when the TSMPIIS moves in the CCD row direction, each target plot's interferogram can be obtained with the same OPD range and the OPD is uniformly-spaced. This is great helpful to sample interference data and reconstruct spectrum.

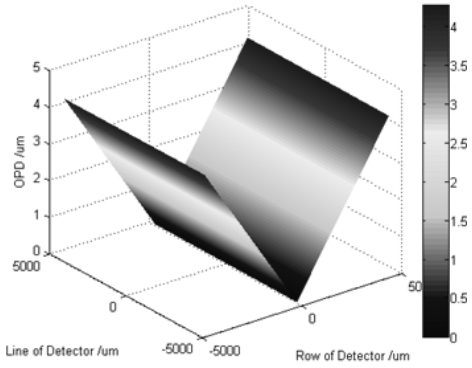

Fig. 3. Optical path difference distribution on the detector of WPIIS at wavelength of 632nm

#117640 - $15.00 USD Received 24 Sep 2009; revised 13 Jan 2010; accepted 13 Jan 2010; published 5 Mar 2010

5. Data processing of TSMPIIS

In traditional Fourier Transform spectroscopy, the basic equation of spectrum and interferogram is defined as:

$$B(\sigma) = \int_{-\infty}^{+\infty} [I(\delta) - \frac{1}{2} I(0)] e^{-i2\pi\sigma\delta} d\delta \qquad (2)$$

where $B(\sigma)$ is known as the spectrum intensity, $I(\delta) - 1/2I(0)$ is the interferogram. So Eq. (2), at a given wave number σ, states that if the flux versus optical path $I(\delta)$ is known as a function of optical path different δ, the Fourier transform of $I(\delta) - 1/2I(0)$ yields $B(\sigma)$, the flux density at the wave number σ. In order to obtain the whole spectrum, it is only need to repeat the calculation of the Fourier transform using Eq. (2) for each wave number in the range of interest. The Fourier Transform theory is perfect without doubt, but in practical applications just as the TSMPIIS, the OPD variety is due to the birefringence effect, which means different wave numbers have different optical path differences, then the theory will be not so accurate. Taking Calcite Crystals as example, and using the OPD Eq. (1), the different maximal OPD of each wave length is obtained as Fig. 4 shows:

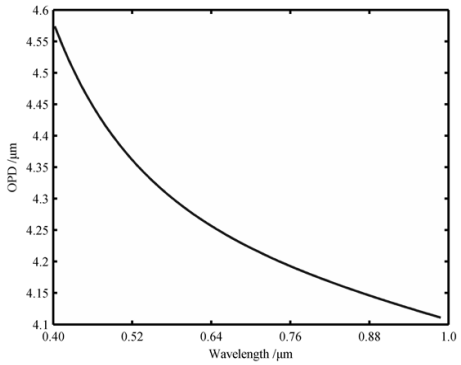

Fig. 4. Maximal optical path difference distribution of TSMPIIS at the wavelength range of 0.4-1.0μm

In Fig. 4, it is easy to find that the maximal OPD is decreased with the wavelength, and the biggest difference between these maximum OPD is about 0.5μm, almost 12% of the maximum OPD at 1.0μm. It means that the OPD sample step $d\delta$ in Eq. (2) for each wave number is quite different. However, usually the obtained interferogram intensity $I(\delta)$ is the omnidirectional intensity contained a range of wave numbers. In this case, it is obviously not accurate to consider the $B(\sigma)$ as the true spectrum when it is the result of the Fourier transform of the detected interferogram intensity $I(\delta)$. In this case, the birefringence interference transform can be used to solve this problem [12]. Below is the detailed analysis and experiment.

Our experimental TSMPIIS uses a 12mm x 12mm x (6 + 6) mm Savart polariscope, a Mintron 512×512 CCD camera, the size of each pixel is 10×10 μm ^{2},and the field of view is $i \approx 3°$. Firstly, according to the interferogram forming principle of the TSMPIIS, we need to sample a target's all interferogram intensity $I(\delta)$ from a series CCD images just like Fig. 5 shows. Figure 5(a) is the image when the target (the rightmost column of Fig. 5(a)) coming into the field of view of TSMPIIS. Figure 5(b)-(e) are the target plot's several images at different position in the field of view of TSMPIIS. Figure 5(f) is the image when the target leaving out of the field of view of TSMPIIS.

#117640 - $15.00 USD Received 24 Sep 2009; revised 13 Jan 2010; accepted 13 Jan 2010; published 5 Mar 2010

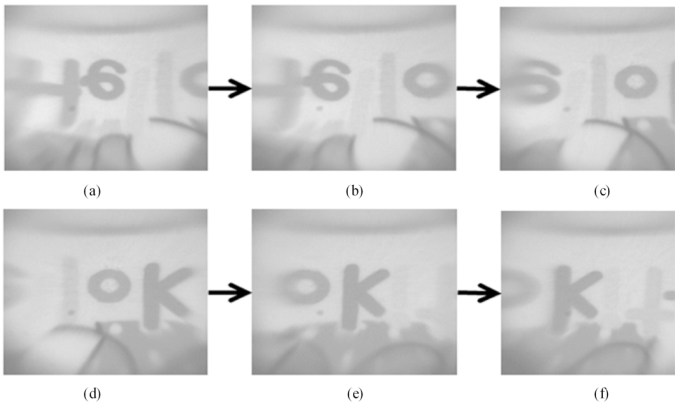

Fig. 5. A target's representative interferogram and images obtained by TSMPIIS under TSM model

To see clearly, Fig. 6 shows a scene's typical enlarged interference fringe and image under white light obtained by TSMPIIS at one moment. Then, sample one target plot's interference data on each frame respectively and organized them regularly from Fig. 5, finally a target's whole interferogram Fig. 7 is got.

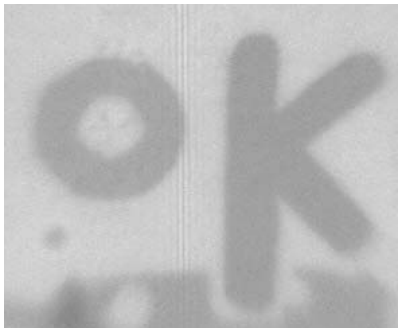

Fig. 6. One enlarged interferogram and image

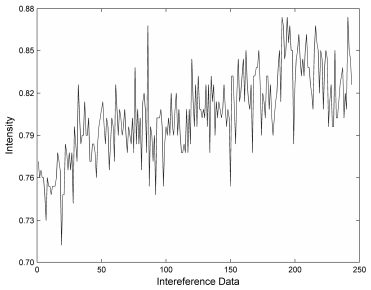

Fig. 7. A target's all interference data of polychromatic light detected by TSMPIIS

In our situation, a target plot's interferogram is consisted of 250 interference data with different optical path differences, and because the light wave with different wave lengths is incoherent light, the detected interferogram intensity $I(\delta)$ is the summation of total waves, just as Eq. (3) shows:

#117640 - $15.00 USD Received 24 Sep 2009; revised 13 Jan 2010; accepted 13 Jan 2010; published 5 Mar 2010

$$\begin{bmatrix} I_{\lambda 1}^{0} \\ I_{\lambda 1}^{1} \\ I_{\lambda 1}^{2} \\ . \\ . \\ I_{\lambda 1}^{250} \end{bmatrix} + \begin{bmatrix} I_{\lambda 2}^{0} \\ I_{\lambda 2}^{1} \\ I_{\lambda 2}^{2} \\ . \\ . \\ I_{\lambda 2}^{250} \end{bmatrix} + \begin{bmatrix} I_{\lambda 3}^{0} \\ I_{\lambda 3}^{1} \\ I_{\lambda 3}^{2} \\ . \\ . \\ I_{\lambda 3}^{250} \end{bmatrix} + ... + \begin{bmatrix} I_{\lambda 250}^{0} \\ I_{\lambda 250}^{1} \\ I_{\lambda 250}^{2} \\ . \\ . \\ I_{\lambda 250}^{250} \end{bmatrix} = \begin{bmatrix} I_0 \\ I_1 \\ I_2 \\ . \\ . \\ I_{250} \end{bmatrix} \tag{3}$$

where $I_{\lambda n}^{0}, I_{\lambda n}^{1}, \ldots, I_{\lambda n}^{250}$ are the interference intensities of each light wave with different OPD, I_0 , I_1 ,.., I_{250} are a target's whole interference intensities showed in Fig. 7. In addition, because $I_{\lambda n}^{0}$, $I_{\lambda n}^{1}$, …, $I_{\lambda n}^{250}$ are the same light wave's interference intensities, their relationship is like that:

$$I_{\lambda n}^{m} = I_{\lambda n}^{0}(1+\cos\Delta_m)/2 \qquad (n = 0,1,2,...,250;\ m = 0,1,2,...,250) \tag{4}$$

where $I_{\lambda n}^{0}$ is the intensity when the OPD is zero, equals to each incident light wave's original intensity of target. Δ_m is the OPD related to each light wave which is calculable and determined by design. Then Eq. (3) can be written as:

$$\begin{bmatrix} 1 & 1 & ... & 1 \\ K_1^1 & K_2^1 & ... & K_{250}^1 \\ K_1^2 & K_2^2 & ... & K_{250}^2 \\ . & & & \\ . & & & \\ K_1^{250} & K_2^{250} & ... & K_{250}^N \end{bmatrix} \begin{bmatrix} I_{\lambda 1}^{0} \\ I_{\lambda 2}^{0} \\ . \\ . \\ . \\ I_{\lambda 250}^{0} \end{bmatrix} = \begin{bmatrix} I_0 \\ I_1 \\ . \\ . \\ . \\ I_{250} \end{bmatrix} \tag{5}$$

where $K_n^0, K_n^1, \ldots, K_n^{250}$ are constant coefficients, and equal to $(1+\cos\Delta_m)/2$. Resolving Eq. (5), the original intensity $I_{\lambda 1}^{0}, I_{\lambda 2}^{0}, \ldots, I_{\lambda 250}^{0}$ of each light wave is obtained. As is well known, the spectrum referred to a plot of light intensity or power as a function of wavelength, also known as a spectral density. So the spectrum that equals to ($I_{\lambda 1}^{0}, I_{\lambda 2}^{0}, \ldots, I_{\lambda 250}^{0}$) is finally got without Fourier transforms as Fig. 8 shows. Its resolution is about 3 nm. The reconstructed spectrum is obviously better than the result of the traditional Fourier Transform which we have presented before [13].

#117640 - $15.00 USD Received 24 Sep 2009; revised 13 Jan 2010; accepted 13 Jan 2010; published 5 Mar 2010

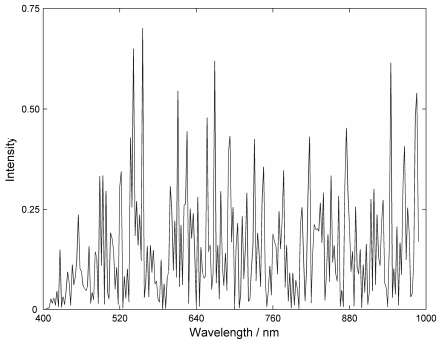

Fig. 8. Reconstructed spectrum of the polychromatic light

6. Conclusions

1. According to the interferogram imaging theory of TSMPIIS, it is known that the TSMPIIS is working under a new model, it can get all detected target plots' interferogram data at one time, but each plot produces only one interference data in one image. A target's whole interferogram is the regular combination of interference data from serial sequential images at different time.

2. Based on analyzing the basic theory of Fourier Transform Spectroscopy, for avoiding the OPD sample step error caused by birefringence crystals, a new processing method is presented. In this method, each light wave's interferogram and intensity are calculated and reconstructed respectively. The final target spectrum is the combination of all light waves without Fourier transforms.

3. The experimental results prove that the temporally and spatially mixed model theory and the data processing method are very efficient to process the data of TSMPIIS。

However, there are still several factors have to be considered carefully in this new data processing method. First of all, the noise will become an assignable cause to the accuracy of final reconstructed spectrum. Because the noise error will great influence the result in calculating each light wave's intensity at zero OPD. So it's important to reduce the system noise as much as possible. Besides this, it will take much more time to count with the computer without a fast algorithm routine like FFT (fast Fourier transform). Of cause, in the other side, there are many potential merits in this new method, such as high accuracy, high spectrum resolution, and simple spectrum calibration. In addition, this method is also suitable for other temporally and spatially mixed modulated spectrometers, too. The only different work to do is to sample the interference data according to their OPD distribution respectively.

Acknowledgements

The authors gratefully acknowledge the support of the State key Program of National Natural Science of China (Grant No. 40537031), National High Technology Research Development Special Fund (863 Project) of China (Grant No. 2006AA12Z152), National Defense Basal Scientific Research Foundation of China (Grant No. A1420080187), the National Natural Science Foundation of China (Grant No. 40875013, 40375010, 60278019).

#117640 - $15.00 USD Received 24 Sep 2009; revised 13 Jan 2010; accepted 13 Jan 2010; published 5 Mar 2010